MATHEWS

Research Article

Mathews Journal of Case Reports

Cytokine-Induced Neurogenesis in Charcot-Marie-Tooth neuropathy with Connexin 32 Gene Mutation

Takuji Shirasawa[1,2,*], Luis Carlos Aguilar Cobos[3]

[1]*Ochanomizu Health and Longevity Clinic, Tokyo, Japan*

[2]*Shirasawa Anti-Aging Medical Institute, Tokyo, Japan*

[3]*Livant Neurorecovery Center, Guadalajara, Mexico*

ABSTRACT

Charcot-Marie-Tooth (CMT) neuropathy is one of the most common neuromuscular disorders. Despite the identification of more than 100 causative genes, there are few therapeutic options. We present the case of a 66-year-old man carrying a CMT mutation in the connexin 32 gene with the APOE genotype ε4/ε3 that had exhibited symptoms of slowly progressive muscle weakness and atrophy in the hands and feet and recently developed memory impairment. The muscle weakness, motor dysfunction, and memory impairment symptoms were significantly improved by cytokine-induced neurogenesis combined with physical wave therapy using an arbitrary waveform generator (AWG). Here, we discuss the possible mechanistic basis of how this new treatment ameliorates the symptoms of CMT and propose a novel clinical treatment strategy for CMT.

Keywords: Charcot-Marie-Tooth (CMT) neuropathy, cytokine, wave therapy, neurogenesis, connexin 32

INTRODUCTION

Charcot-Marie-Tooth (CMT) neuropathy is one of the most common neuromuscular disorders [1]. The estimated frequency of CMT is 1 in 2,500 individuals [2]. CMT is differentially classified according to the age of onset, type of inheritance and clinical features [2]. Mutations in more than 100 genes have been implicated as causal factors, with mutations in PMP22 being one of the most common [2]. The major demyelinating type (CMT1) affects more than 30% of CMT patients and manifests as motor and sensory dysfunction of the peripheral nervous system that begins with slow progressive weakness of the lower extremities in most cases. The X-linked dominant form of CMT (CMTX) is caused by mutations in the connexin 32 (CX32) gene, mapped to Xq13, which encodes a gap junction protein [3]. It has been suggested that CX32 is enriched in the nodes of Ranvier in Schwann cells and plays an important role in neurotransmission in peripheral nerves [4]. Since connexin 32 is a component of gap junction channels, the mutation found in CMTX patients may disturb the channel function in gap junctions of peripheral nerves [4]. Despite the identification of more than 100 causative genes,

Vol No: 08, Issue: 07

Received Date: May 12, 2023

Published Date: June 01, 2023

***Corresponding Author**

Takuji Shirasawa

Shirasawa Anti-Aging Medical Institute, Sagawa BLD 701, KandaSurugadai 2-8, Chiyoda-Ku, Tokyo 101-0062, Japan

Email: shirasawa@shirasawa-acl.net

Citation: Shirasawa T, et al. (2023). Cytokine-Induced Neurogenesis in Charcot-Marie-Tooth neuropathy with Connexin 32 Gene Mutation. Mathews J Case Rep. 8(7):118.

there are few therapeutic options [1]. Current management, thus, relies on rehabilitation therapy, surgery for skeletal deformities, and symptomatic treatment of pain, fatigue and cramps, complaints which are both frequent and difficult to treat [5]. In the present study, we showed for the first time the most promising clinical strategy to improve the symptoms of CMT: cytokine-induced neurogenesis combined with physical wave treatment.

CASE PRESENTATION

A 66-year-old Japanese man visited our clinic for muscle weakness and memory dysfunction on March 25, 2019. The patient had a history of slowly progressive distal limb-dominant muscular dystrophy with muscle weakness and muscle atrophy. He had no family history of muscular dystrophy or any hereditary disorders. He visited the University of Tokyo Hospital to obtain a diagnosis of muscular dystrophy in 2003, where sequence analysis of causative genes for CMT, including connexin 32, P0, and PMP22, revealed that a mutation was found in codon 26 in exon 2 of the connexin 32 gene, in which TCG was replaced by TTG, causing an amino acid change from Ser to Leu (Figures 1B, 1C). He reported moderate muscle atrophy in both hands and feet that required ankle-foot orthosis for smooth walking.

The patient also developed gradual progression of memory dysfunction with well-preserved language comprehension, emotional control, and spatial and temporal orientation. At his first visit to our clinic on March 25, 2019, his score (28/30) on the Mini-Mental State Examination (MMSE) indicated minimal cognitive impairment with mild memory impairment. His emotional control and language comprehension were well preserved. Apoprotein E (APOE) genotype analysis showed that he was an ε4/ε3 heterozygous carrier. Cognitive function examination using Cognitrax at his first visit revealed verbal memory impairment (Cognitrax score=69), while his reaction times, motor speed, sustained attention, cognitive flexibility, executive function, reasoning, and working memory were normal (Figure 2). MRI data acquired at his first visit, showed moderate atrophy of the cerebral cortex in the parietal lobes and mild atrophy in the frontal and temporal lobes (Figure 3A). A cross-sectional cortical image of the precentral and postcentral gyri of the left central cerebral cortex revealed reductions in both gray matter and white matter volumes, with enlarged sulci and degenerated cortical structures (Figure 3C). Interestingly, the volume of the motor cortex (precentral) was relatively preserved compared with that of the sensory cortex (postcentral), suggesting compensatory hyperplasia due to CMT (Figures 3A, 3C). MRA data acquired at his first visit showed moderate degenerative changes in the distal branches from the left MCA M2 branches as well as the left PCA branches (Figure 3E). Similar degenerative changes were also observed in the right MCA and PCA branches. EEG data analyzed by Neuroscan Software to reveal the P300 showed that after a repeated stimulus (low-pitched sound), P300 responses were globally suppressed at the frontopolar, frontal, central, temporal, parietal, and occipital electrodes (Figure 4A, red lines), suggesting that degenerative pathology such as Alzheimer's disease underlies the observed cerebral atrophy. At the left frontal electrode, we detected an abnormally flattened P300 response with a lower voltage of 5 μV^2 (Figure 4B, red line in left panel). The right frontal electrode also showed a similar abnormal flattened P300 response (Figure 4B, red line in right panel), suggesting a global degenerative pathology in the frontal, temporal, parietal, and occipital lobes. As shown in Figure 4C, P300 coherence analysis showed abnormal coherence of high and low frequency fluctuations in the F3 (left frontal) and F4 electrodes (right frontal) (Figure 4C, indicated by red arrows), suggesting a deficiency of inhibitory GABAergic interneurons in the frontal lobes. As shown in Figure 4D, emotional control analysis showed that all evaluated emotions, namely, joy, sadness, happiness, neutral feeling, and anxiety, were depressed in both left frontopolar electrodes (Figure 4D, left panel), implying that there was degenerative pathology in the frontal lobe or that the dopaminergic projections to the frontal lobe were down regulated. Blood chemistry, CBC, and HbA1c analyses failed to indicate any disorders associated with dementia or muscular dystrophy-related diseases. We therefore diagnosed this patient with CMT complicated with Alzheimer's disease.

We treated the patient with a cytokine cocktail containing hepatocyte growth factor (HGF), granulocyte colony stimulating factor (GCSF), adiponectin, insulin-like growth factor-1 (IGF-1), and IGF-2 from March 25, 2019, to July 08, 2020 (Figure 2, lower panel). We then supplemented the treatment with additional cytokines, vascular endothelial growth factor (VEGF), progranulin and brain tissue-derived exosomes from July 08, 2020, to January 15, 2022 (Figure 2, lower panel). The clinical protocol used in this study as well as the cytokine cocktail formulation was designed and developed by Luis Carlos Aguilar Cobos at the Livant Neurorecovery Center, Mexico as described previously [6].

On January 15, 2022, 34 months after cytokine cocktail treatment, the patient's verbal memory function, which had previously been impaired, exhibited recovery, with a concomitant improvement in MMSE score (from 28/30 to 30/30) (Figure 2). The patient's cognitive functions further improved in terms of cognitive flexibility, executive function, working memory, attention, reasoning, reaction time, motor

speed, and verbal memory, as illustrated in Figure 2.

In order to take care of the muscle weakness caused by CMT, we regularly stimulated the muscles of the upper and lower extremities with waves of a specific frequency generated by an arbitrary waveform generator (AWG) every month (Ajax AWG, https://www.awg-wave.co.jp/en/awg-oc/). Although the patient still showed muscle atrophy at the base of the thumb on April 14, 2023 (Figure 1A) as well as in both his feet, although his ADL (activity of daily living) improved in association with the maintenance of muscle strength and motor functions such as grasping a pen or chopsticks or walking without orthopedic cast.

We reevaluated the patient's EEG activity, and P300 EEG responses were significantly improved, showing a higher amplitude and symmetrical response in all brain areas, including the frontal, temporal, parietal, and occipital lobes (Figure 4A, black lines). These restored responses suggest that both inhibitory GABAergic interneurons and excitatory glutamatergic neurons were successfully globally regenerated to reconstruct the functional neuronal networks in the cerebral cortex, as suggested previously [6-7]. Higher amplitude of P300 responses at the left frontal electrode clearly showed that the low-amplitude P300 observed before treatment significantly improved to a normal P300 response at a 240 ms latency with a 17.50 μV^2 amplitude after treatment (Figure 4B, black line in left panel). Another improvement was observed in the right frontal electrode (Figure 4B, right panel). Coherence analysis showed normal P300 coherence of the left and right frontal electrodes with normal fluctuations (Figure 4C, right panel indicated by arrows). The depressed emotional reactions recorded on March 25, 2019, had significantly improved on January 15, 2022 (Figure 3D), indicating that cytokine-induced neurogenesis and angiogenesis were physiologically relevant for the processing of dopaminergic projections to the frontal lobes.

We performed MRI on February 14, 2022, which showed a significant increase in the volume of the atrophied precentral and postcentral gyri in the frontal and parietal cortex after treatment (Figure 3B). The cross-sectional image of the recovered gyri showed increased gray matter and white matter volumes with enlarged gyri and normal cortical structure (Figure 3D). MRA data collected on February 14, 2022 clearly showed significant angiogenesis of the MCA branches and PCA branch (Figure 3F), suggesting that the improvement in blood supply induced not only the regeneration of damaged brain tissue but also rescued neurophysiological activity for normal cognitive function [8].

DISCUSSION

In the present case report, we demonstrate for the first time that cytokine therapy combined with physical wave therapy with an AWG constitutes a novel treatment protocol for CMT. The improvement in symptoms included the reversal of cognitive decline in working memory, verbal memory, attention, cognitive flexibility and executive function, possibly due to Alzheimer's disease, along with the amelioration in motor dysfunction of the upper and lower extremities due to CMT.

To analyze the structural abnormality of mutant connexin 32 S26L, we simulated the molecular structure of mutant connexon composed of connexin 32 S26L in silico using SWISS-MODEL (https://swissmodel.expasy.org) with CX43 (PDF ID: 7F94, https://www.rcsb.org/structure/7F94) [9] as the template [10]. As shown in Figure 5A, the differences between the wild-type and mutant connexon S26L clearly suggests that the mutation S26L could alter the tertiary structure of the connexon with open structure or open-closed transition in gap junctions, as illustrated in Figure 5C. Since the mutated Leu residue is localized to the interface between connexin 32 chains (Figure 5B), it is reasonable to speculate that the mutant connexon fails to open or close properly such that the gap junction channel does not allow small molecules to pass through because of structural abnormalities in the pore structure of mutant connexon S26L (Figure 5C).

We applied an arbitrary waveform generator (AWG) for the treatment of CMT in the present study. Extracorporeal shock wave therapy (ESWT) is popular for treating neurological diseases, including central and peripheral nervous system diseases [11]. However, use of an AWG is quite different from ESWT because (1) the AWG emits an alternating current signal with one of 111 distinct frequencies from 1 to 10,000 Hz, and (2) the AWG stimulates tissues with a program that provides various cycles of interval emission of 3-min duration from low frequency to high frequency (Ajax AWG, https://www.awg-wave.co.jp/en/awg-oc/). Thus, intriguingly, on the physiological cellular level, the frequency of waves emitted by AWG may rectify the dysfunction of channel properties caused by mutant connexin 32 S26L in gap junctions for molecules smaller than 1000 Da, such as cAMP [12]. Alternatively, AWG may stimulate other physiological gap junction channels composed of different connexin isoforms to rectify the abnormal channel properties caused by gene mutation [13]. Interestingly, electrical stimulation (ES) at 20 Hz for 1 h has been shown to ameliorate intracellular PMP22 (peripheral myelin protein 22) aggregation and return the PMP22 distribution to healthy conditions in PMP22-overexpressing Schwannoma cells in an in vitro model of CMT1A [14]. The authors suggested that enhanced gene

expression of myelin basic protein (MBP), myelin-associated glycoprotein (MAG), myelination-regulating transcription factors Krox-20, Oct-6, c-Jun, and Sox10 provided mechanistic insight into the efficacy of ES [14].

The neurophysiological study suggested that GABAergic inhibition is suppressed in the motor area of the frontal cortex, as shown in P300 coherence analysis (Figure 4C), resulting in hyperexcitability of glutamatergic neurons to compensate for the degeneration of downstream peripheral neurons. A similar pathophysiology is well documented in chemotherapy-induced peripheral neuropathy (CIPN) [15]. In this study of CIPN, the authors emphasized that the pathological role of the brain in peripheral neuropathy involves (1) brain hyperactivity, (2) reduced GABAergic inhibition, (3) neuroinflammation, and (4) overactivation of GPCR/MAPK pathways [15]. As the patient is an APOE ε4/ε3 heterozygous carrier, accumulated amyloid-ß can also inhibit GABAergic interneurons as described previously [6]. The cytokine cocktail treatment induced GABAergic and glutamatergic neurogenesis (Figure 3D), reconstructing a normal cortical neuron network (Figure 4B) to compensate for the downstream peripheral neuropathy.

CONCLUSION

Charcot-Marie-Tooth (CMT) neuropathy is one of the most common neuromuscular disorders. Despite the identification of more than 100 causative genes, there are few therapeutic options. In the present case study, we demonstrate that the combination of cytokine-induced neurogenesis with physical wave therapy by an arbitrary waveform generator (AWG) is currently the most promising treatment option for CMT.

ACKNOWLEDGEMENTS

The authors thank Ms. Sayuri Sato, Ms. Masami Fukuda, and Ms. Fernanda Diaz for assistance in the preparation of this manuscript.

INFROMED CONSENT

Written informed consent was obtained from the patient.

CONFLICT OF INTEREST

The authors declare that they have no conflicts of interest.

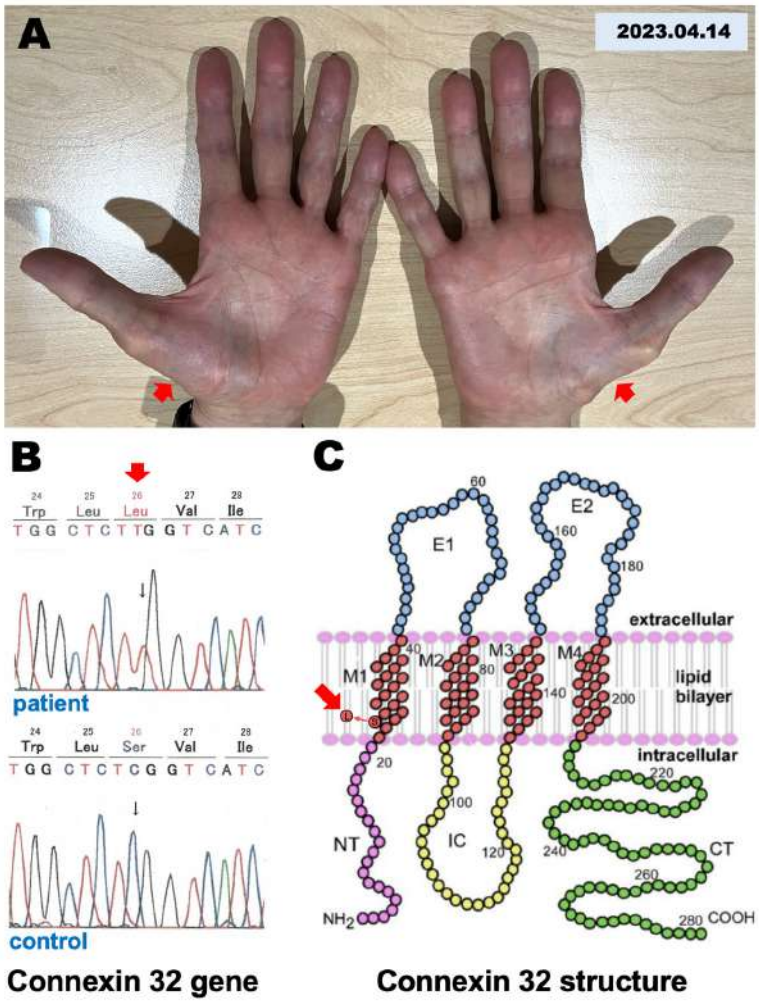

Figure 1: Muscular dystrophy and mutation in the connexin 32 gene.

A. A photomicrograph of hands shows muscular dystrophy in the base of both thumbs recorded on April 14, 2023.

B. A mutation was found in the connexin 32 gene that causes an amino acid change from Ser to Leu in the 26th amino acid sequence of connexin 32.

C. A mutation was found in the TM1 domain of the connexin 32 secondary structure.

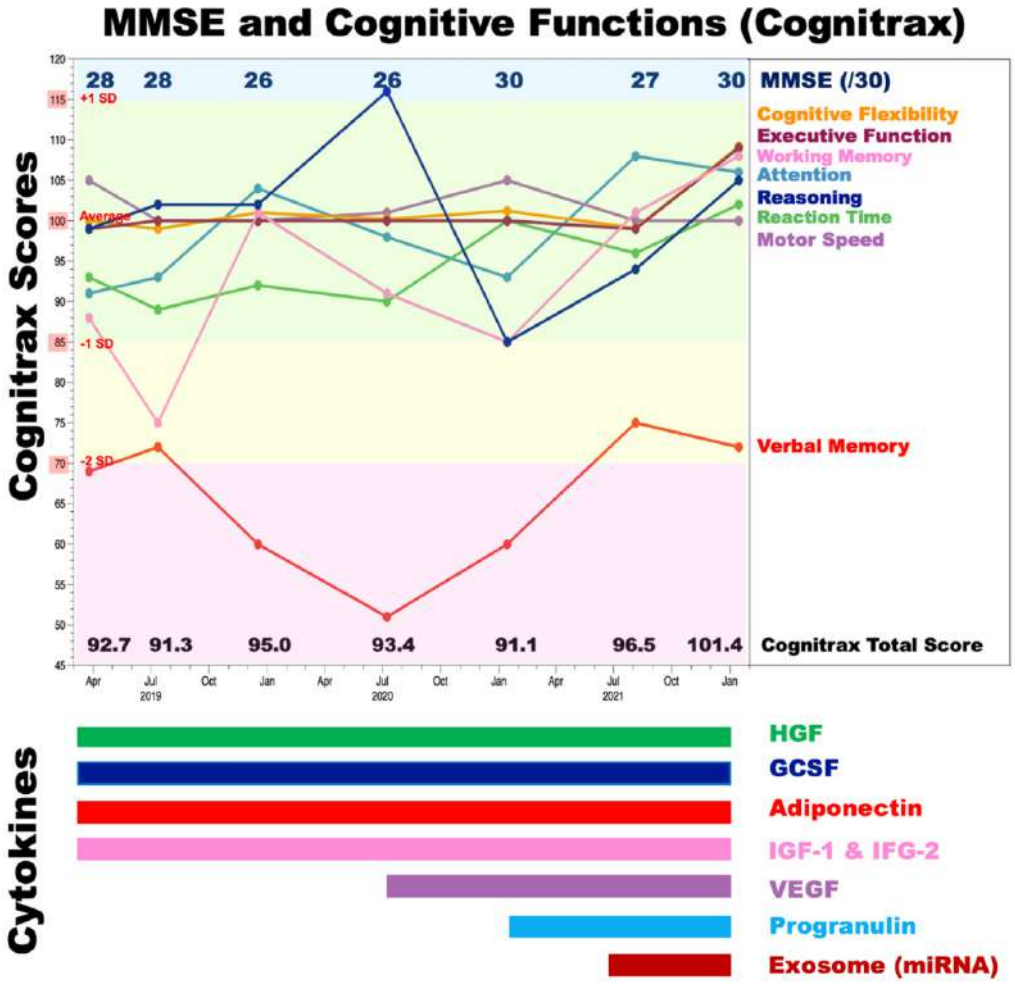

Figure 2: MMSE scores and cognitive function before and after cytokine-induced neurogenesis.

Cognitive functions were evaluated by Cognitrax and the Mini-Mental State Examination (MMSE) at five timepoints: March 25, 2019, July 12, 2019, December 17, 2019, July 8, 2020, January 14, 2021, August 10, 2021, and January 15, 2022. The MMSE scores are shown in the upper part of the graph. Cognitrax scores for cognitive flexibility (orange), executive function (brown), working memory (magenta), attention (light blue), reasoning (dark blue), reaction time (green), motor speed (plum), and verbal memory (red) are shown chronologically. A Cognitrax score of 100 is the average score among the Japanese population of the same age. Green indicates the zone of the average ± 1 SD, yellow indicates the zone from 1 SD to 2 SD less than the average, red indicates the zone more than 3 SD less than the average, and blue indicates the zone + 1 SD over the average. Administered cytokines and exosomes are shown under the graph.

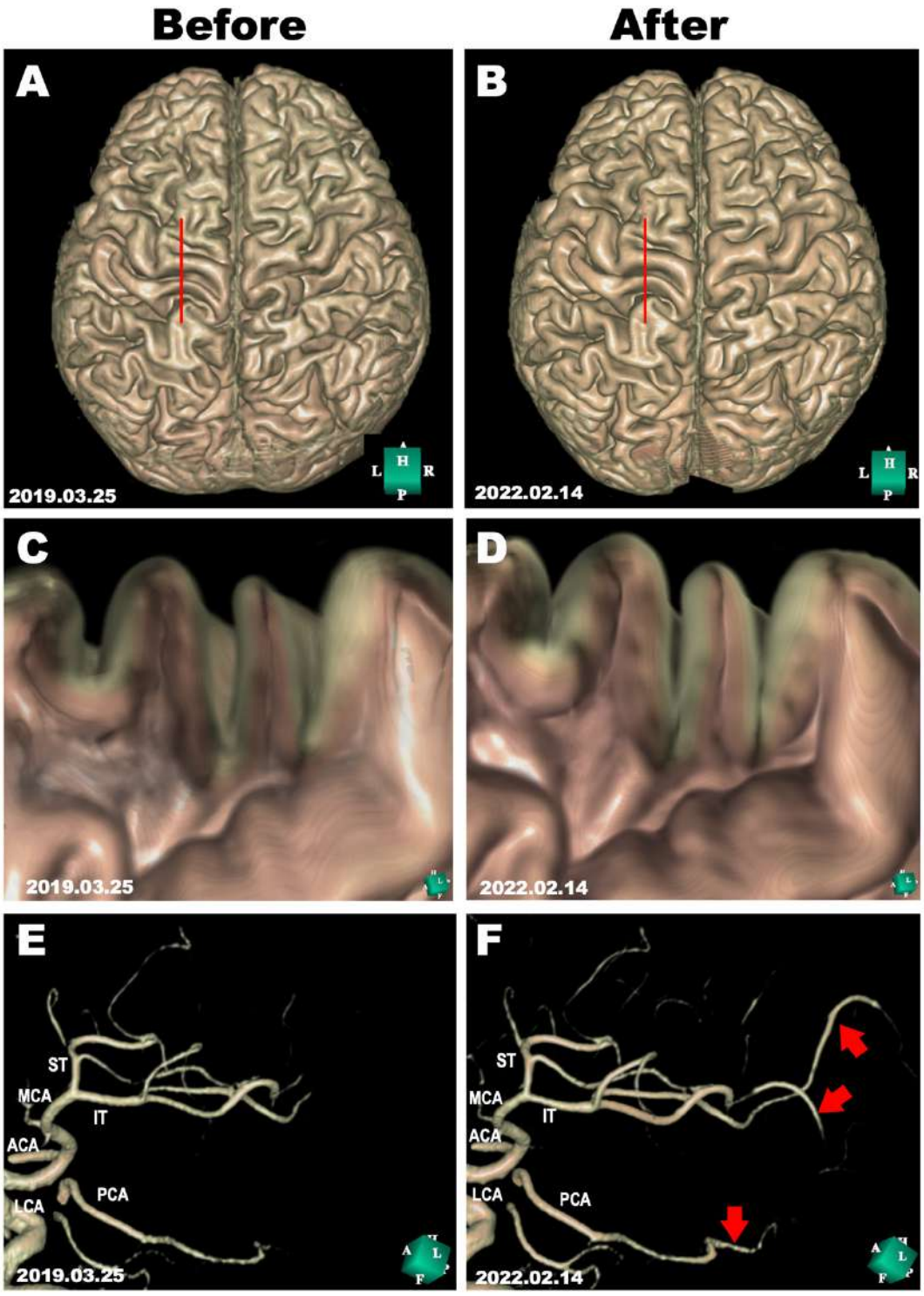

Figure 3: Morphological evaluations before and after cytokine-induced neurogenesis.

MRI scans were performed on March 25, 2019, and on February 14, 2022, before and after cytokine cocktail treatment. A, B: 3D structure of the cerebral cortex reconstructed in silico using Expert INTAGER software from MRI T1-weighted images with 1-mm sagittal slices before and after cytokine cocktail treatment. C, D: Cross-sectional images of the motor area in the left frontal lobe (as indicated by red lines in A and B) show the regeneration of the atrophied cerebral cortex. E, F: The left middle cerebral artery (MCA) branches and posterior cerebral artery (PCA) before and after cytokine cocktail treatment. Regenerated MCA and PCA branches are indicated by red arrows. ACA, anterior cerebral artery; IT, inferior trunk of MCA; LCA, left carotid artery; MCA, middle cerebral artery; PCA, posterior cerebral artery.

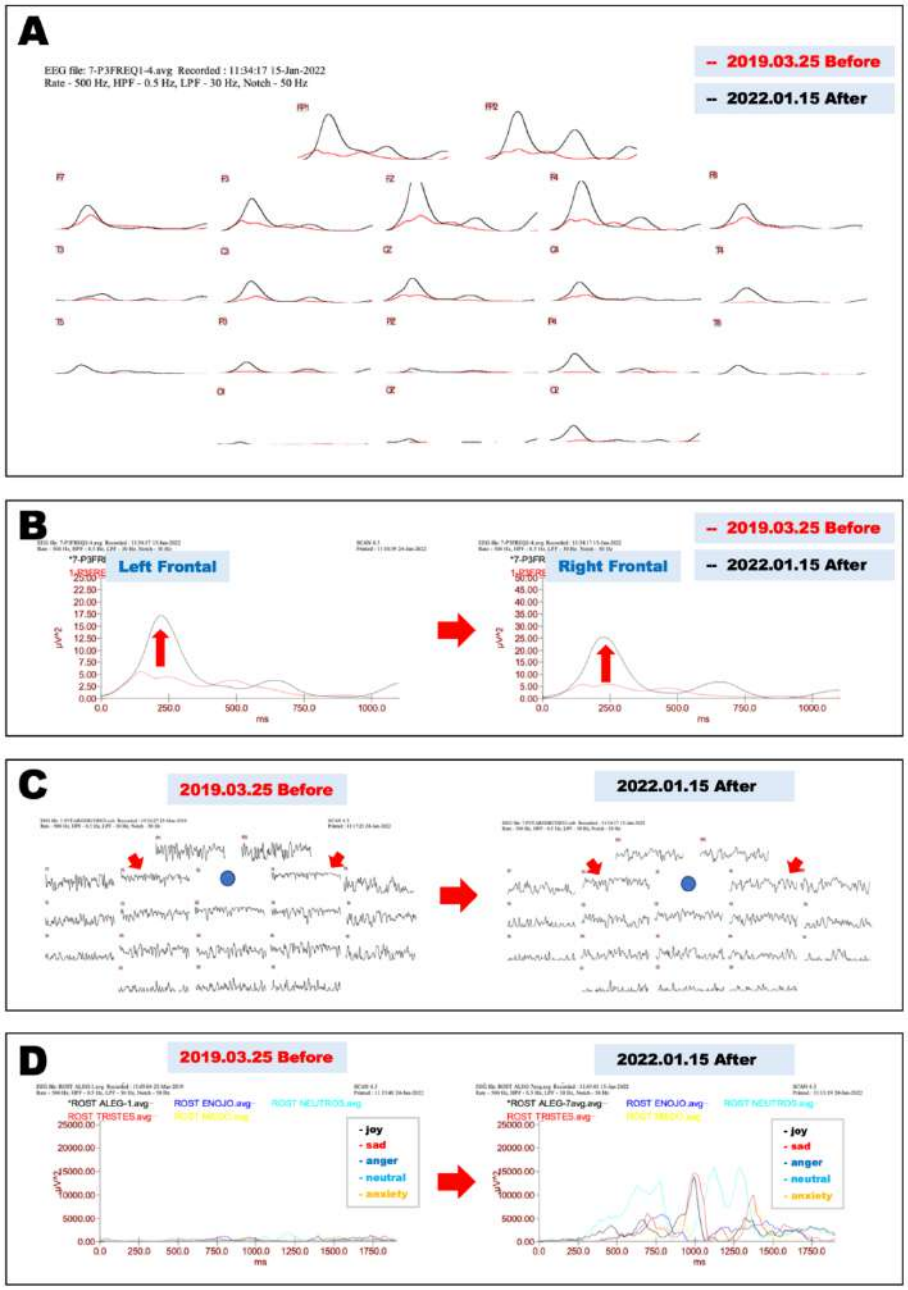

Figure 4: Neurophysiological evaluations before and after cytokine-induced neurogenesis.

A. Electrophysiological evaluation of P300 EEG responses before and after cytokine-induced neurogenesis. Before-treatment (March 25, 2019) P300 EEG responses after a repeated stimulus (low-pitched sound) are shown as red lines; after-treatment (January 15, 2022) EEG responses are shown as black lines.

B. Magnified view of recordings from frontal electrodes in Fig. 4A show that the asymmetrical P300 recorded on March 25, 2019 (red lines) significantly improved and became symmetrical in recordings from both frontal electrodes on January 15, 2022 (black lines; left, left frontal leads; right, right frontal leads).

C. Coherence analysis of P300 before and after cytokine-induced neurogenesis. Impaired neural network connections recorded on March 25, 2019, in frontal electrodes (F3 and F4, as shown by red arrows) were significantly improved on January 15, 2022.

D. Emotional control analysis before and after cytokine-induced neurogenesis. EEG recordings at the left frontopolar electrode while watching a happy face (black), sad face (red), angry face (blue), expressionless face (light blue), and worried face (yellow) recorded on March 25, 2019 (left panel), or on January 15, 2022 (right panel).

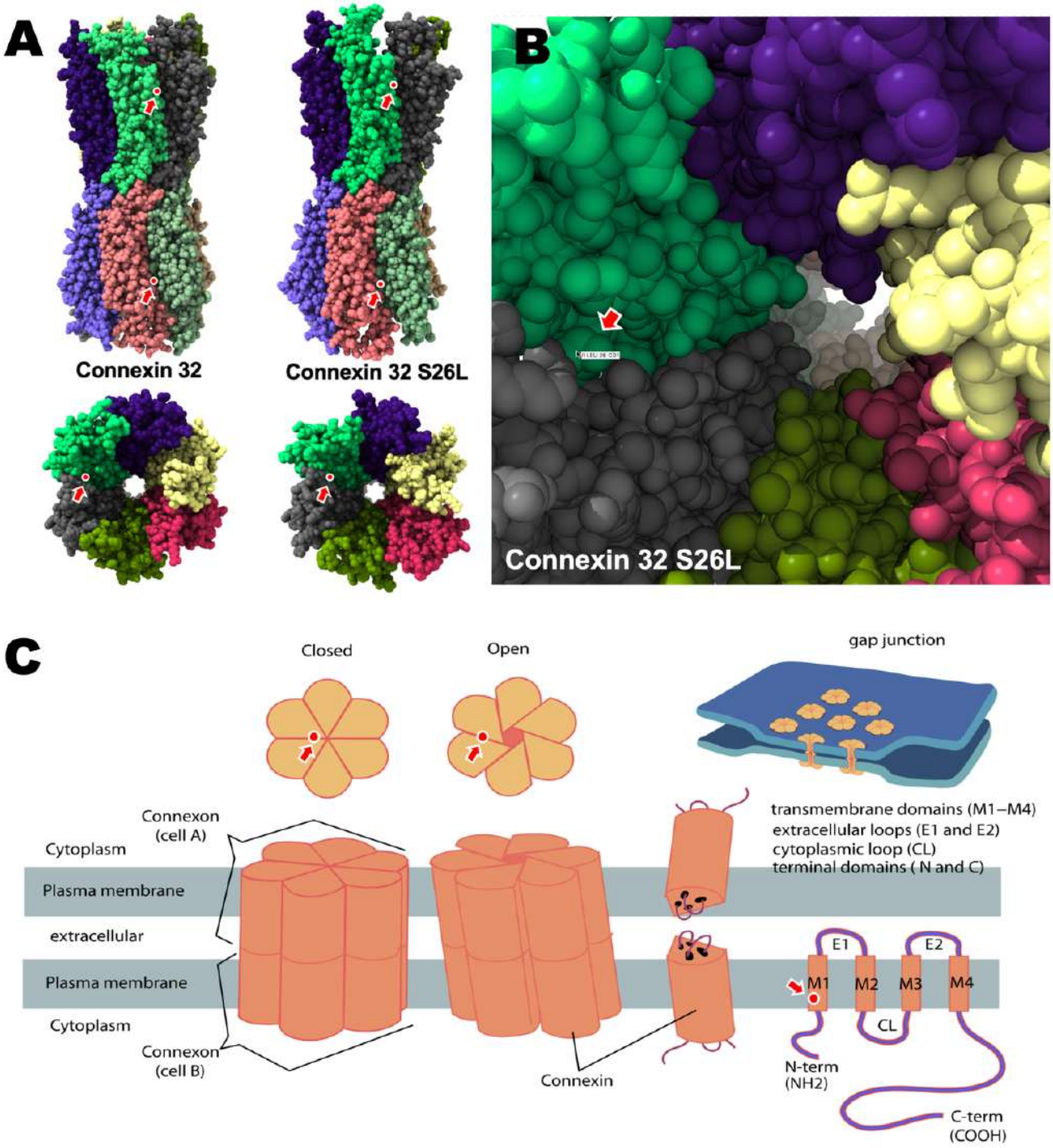

Figure 5: Structural alteration of the connexin 32 S26L mutant.

A. Homology modeling of connexin 32 and the connexin 32 S26L mutant shows that the mutation is localized to the interface of connexin 32 chains, as indicated by arrows.

B. Higher magnification view of the channel pore in the gap junction shows that the mutated amino acid Leu26 is localized to the inner interface between connexin chains of mutant connexin 32 S26L.

C. Graphic illustration of the closed and open barrel structures of the connexon molecule composed of 2 sets of 6 connexin chains (modified from Connexon in WIKIPEDIA, https://en.wikipedia.org/wiki/Connexon). The localization of mutant Leu26 is indicated by arrows.

REFERENCES

1. Bolino A, D'Antonio M. (2023). Recent advances in the treatment of Charcot-Marie-Tooth neuropathies. J Peripher Nerv Syst. 1-16.
2. Comella M, Collotta A, Pavone V, Ciccia L, Bellinvia A, Cerruto C, et al. (2022). Concomitant MPZ and MFN2 Gene Variants and Charcot Marie Tooth Disease in a Boy: Clinical and Genetic Analysis-Literature Review. Case Rep Pediatr. 2022:1-6.
3. Wicklein EM, Orth U, Gal A, Kunze K. (1997). Missense mutation (R15W) of the connexin32 gene in a family with X chromosomal Charcot-Marie-Tooth neuropathy with only female family members affected. J Neurol Neurosurg Psychiatry. 63(3):379-381.
4. Cisterna BA, Arroyo P, Puebla C. (2019). Role of Connexin-Based Gap Junction Channels in Communication of Myelin Sheath in Schwann Cells. Front Cell Neurosci. 13 69 :61-68.
5. Pisciotta C, Saveri P, Pareyson D. (2021). Challenges in Treating Charcot-Marie-Tooth Disease and Related Neuropathies: Current Management and Future Perspectives. Brain Sci. 11(11):1447.
6. Shirasawa T, Cobos LCA. (2022). Cytokine-induced Neurogenesis for Alzheimer's Disease and Frontotemporal Dementia. Personalized Med Universe. 11(1):27-32.
7. Shirasawa T, et al. (2023). Cytokine-induced Neurogenesis Can Reverse Cognitive Decline in Alzheimer's Disease. Mathews J Case Rep. 8(3):97.
8. Shirasawa T, Cobos LCA. (2023). Cytokine-Induced Neurogenesis and Angiogenesis Reversed Cognitive Decline in a Vascular Dementia Patient with Hashimoto's Thyroiditis. ES J Case Rep. 4(1):1036.
9. Lee HJ, Cha HJ, Jeong H, Lee SN, Lee CW, Kim M, et al. (2023). Conformational changes in the human Cx43/GJA1 gap junction channel visualized using cryo-EM. Nat Commun. 14(1):931.
10. Bordoli L, Kiefer F, Arnold K, Benkert P, Battey J, Schwede T. (2009). Protein structure homology modeling using SWISS-MODEL workspace. Nat Protoc. 4(1):1-13.
11. Guo J, Hai H, Ma Y. (2022). Application of extracorporeal shock wave therapy in nervous system diseases: A review. Front Neurol. 13:963849.
12. Kumar NM, Gilula NB. (1996). The gap junction communication channel. Cell. 84(3):381-388.
13. Schadzek P, Hermes D, Stahl Y, Dilger N, Ngezahayo A. (2018). Concatenation of Human Connexin26 (hCx26) and Human Connexin46 (hCx46) for the Analysis of Heteromeric Gap Junction Hemichannels and Heterotypic Gap Junction Channels. Int J Mol Sci. 19(9):2742.
14. Intisar A, Woo H, Kang HG, Kim WH, Shin HY, Kim MY, et al. (2023). Electroceutical approach ameliorates intracellular PMP22 aggregation and promotes pro-myelinating pathways in a CMT1A in vitro model. Biosens Bioelectron. 224:115055.
15. Omran M, Belcher EK, Mohile NA, Kesler SR, Janelsins MC, Hohmann AG, et al. (2021). Review of the Role of the Brain in Chemotherapy-Induced Peripheral Neuropathy. Front Mol Biosci. 8:693133.